

Direct Numerical Simulations of Fundamental Turbulent Flows with the World's Largest Number of Grid-points and Application to Modeling of Engineering Turbulent Flows

Project Representative

Yukio Kaneda Graduate School of Engineering, Nagoya University

Authors

Yukio Kaneda Graduate School of Engineering, Nagoya University

Takashi Ishihara Graduate School of Engineering, Nagoya University

Kaoru Iwamoto Mechanical Systems Engineering, Tokyo University of Agriculture and Technology

Tetsuro Tamura Interdisciplinary Graduate School of Science and Engineering, Tokyo Institute of Technology

Yasuo Kawaguchi Department of Mechanical Engineering, Tokyo University of Science

Takahiro Tsukahara Department of Mechanical Engineering, Tokyo University of Science

High-resolution direct numerical simulations (DNSs) of canonical turbulence were performed on the Earth Simulator 2. They include (i) high-Reynolds-number turbulent channel flows, (ii) a decaying axisymmetric turbulence, and (iii) turbulent boundary layers on sinusoidal wavy walls. They provide us with invaluable detailed information on the related various turbulence phenomena. The analyses of the DNS data show the following. (1) Intermittent nature of vorticity components is strongly related to the characteristic structures of vorticity near the wall. (2) There is no return to isotropy in a fully developed state of decaying axisymmetric turbulence. (3) The friction coefficient for the TBL with sinusoidal wavy walls differs from that with transverse square bars.

We also performed the following turbulence simulations for environmental and industrial applications. (iv) Application of LES of turbulent flows to urban environmental and strong wind disaster problems, (v) LES of the flow around circular cylinder in realistic high Reynolds number region, and (vi) DNS of turbulent heat transfer of non-Newtonian surfactant solution passing complicated geometry. The results of these simulations show the following. (4) By employing the LES technique for wind flow accompanied with heat around dense tall buildings existing in the urban area we can reproduce the complex flows among many buildings and their wakes with smaller scale. (5) The present LES model succeeded in simulating the aerodynamic characteristics at the critical Reynolds numbers. (6) In a channel flow with rectangular orifices for a viscoelastic fluid, the heat-transfer-reduction rate is lower than the drag-reduction rate, unlike the smooth channel flow.

Keywords: High-resolution DNS, turbulent channel flow, MHD turbulence, turbulent boundary layer, rough wall, LES, urban turbulent boundary layer, critical Reynolds number, non-Newtonian fluid, heat transfer, drag reduction

1. Direct Numerical Simulations of Fundamental Turbulent Flows

1.1 High resolution DNS of turbulent channel flow

To investigate the small-scale statistics in wall-bounded turbulence and to study their Reynolds number dependence, we performed a series of direct numerical simulations (DNS's) of turbulent channel flow (TCF) of an incompressible fluid obeying the Navier-Stokes (NS) equations. The flow is between two parallel flat plates in wall-normal (y) direction, and is assumed to be periodic in the streamwise (x) and span-wise (z) directions.

The computational domain is given by $(2\pi h \times 2h \times \pi h)$, the sizes of which in the x - and z -directions are twice those used in the previous year [1]. Here h denotes the channel half-width. We use the Fourier-spectral method in the x - and z -directions, and the Chebyshev-tau method in the y -direction. The alias errors are removed by the 3/2 rule. Time evolution is accomplished by a third-order Runge-Kutta method for the convection term and the first-order implicit Euler method for the viscous terms. To obtain reliable statistics we advanced each DNS at least until time t larger than $10 t_w$, where t_w is the wash-out time. The

largest-scale DNS (with $2048 \times 1536 \times 2048$ grid points) achieves the sustained performance of 6.1Tflops (11.7% of the peak performance) using 64 nodes of ES2 and generates the DNS data of TCF with the friction Reynolds number $Re_\tau = 2560$. Table 1 shows the parameters used in the series of DNS's.

In TCF, the Kolmogorov length scale $\eta = (\nu / \langle \epsilon \rangle_{xz})^{1/4}$ is a function of the distance (y) from the wall, where ν is the kinematic viscosity, ϵ the rate of energy dissipation and $\langle \cdot \rangle_{xz}$ denotes the average over a plane parallel to the wall. Figure 1 shows that the maximum mesh size in the wall-normal direction in the DNS of the TCF (Case 4) is smaller than the mesh size that was used in the DNS of homogeneous isotropic turbulence by Kaneda et al [2], i.e. $\Delta x / \eta \sim 3$ or 6. This result suggests that we can achieve $Re_\tau = 5120$ by using $2048 \times 1536 \times 2048$ grid points in a smaller computational domain $(\pi h) \times (2h) \times (\pi h/2)$. We have performed such a DNS up to $t = 4.5t_w$ in the fiscal year of 2011.

The preliminary analysis of the series of the DNS data in Table 1 showed that the flatness factor of each component of vorticity depends on the wall-normal distance and strongly relates to the characteristic vortex structures and their distributions near the wall. The DNS data suggest that the flatness factor of a certain component of vorticity at a certain wall-normal distance, which relates to the characteristic vortex structures near the wall, is an increasing function of Re_τ .

1.2 The decay of axisymmetric turbulence

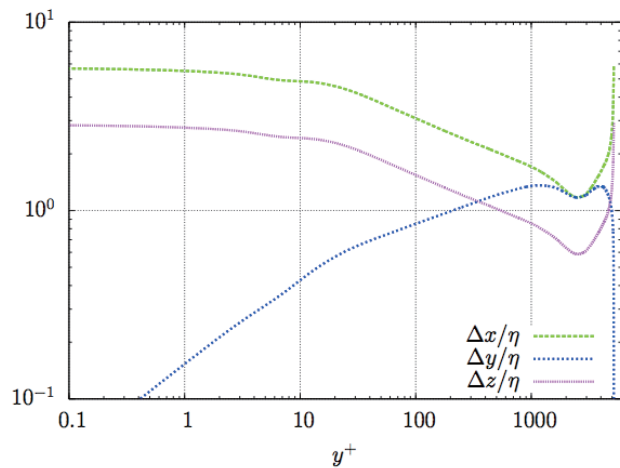


Fig. 1 y -dependence of the mesh size normalized by the Kolmogorov dissipation length scale, used in the DNS of the TCF at $Re_\tau = 2560$ on $2048 \times 1536 \times 2048$ grid points.

Table 1 Parameters used in the DNS's of TCF. Δx^+ and Δz^+ are the mesh size (normalized by u_τ and h) in the streamwise (x) and span-wise (z) directions, and Δy_c^+ is the wall-normal mesh size at the channel center.

	Re_τ	L_x/h	L_z/h	$N_x \times N_y \times N_z$	Δx^+	Δy_c^+	Δz^+
Case 1	320	2π	π	$256 \times 192 \times 256$	7.9	7.9	3.9
Case 2	640	2π	π	$512 \times 384 \times 512$	7.9	7.9	3.9
Case 3	1280	2π	π	$1024 \times 768 \times 1024$	7.9	7.9	3.9
Case 4	2560	2π	π	$2048 \times 1536 \times 2048$	7.9	7.9	3.9

In order to examine the decay of axisymmetric turbulence, we performed direct numerical simulations of freely decaying axisymmetric turbulence at different levels of initial anisotropy with the number of grid points up to 1024^3 on the ES. There are two canonical cases in the decay of freely decaying turbulence. One is $E(k \rightarrow 0) \sim k^2$ and the other is $E(k \rightarrow 0) \sim k^4$, where $E(k)$ is the energy spectrum and k the wavenumber, respectively. We examined the first of these. The DNS's were performed in a periodic domain whose size is sufficiently larger than the integral scales of the turbulence. It is found that there is no return to isotropy in a fully-developed state, irrespective of the level of initial anisotropy, and Saffman's decay laws hold true. Further details are shown in [3].

2. DNS of turbulent boundary layer on rough walls

Turbulent boundary layer on rough plates is one of the most important problems in fundamental turbulent heat transfer research, practical engineering applications and environmental processes. DNS of turbulent boundary layer on rough walls has been barely performed compared with that of other wall-bounded turbulence such as turbulent channel flows.

In this study, direct numerical simulation of turbulent boundary layer with several sinusoidal wavy walls has been performed in order to investigate the effect of the wave length of the sinusoidal wavy wall, λ , upon the turbulent statistics. The amplitude of the sinusoidal wavy wall, a , was kept constant in wall units, and the wave length was set to be $\lambda/a = 5, 7.5, 10, 12.5, 15, 22.5$ and 45 . For the spatially developing boundary layers on sinusoidal wavy walls, we provided a driver section with a flat wall and an analysis section with a sinusoidal wavy wall as shown in Fig. 2. Turbulent inflow conditions for the driver section are generated by rescaling the turbulent boundary layer at some distance downstream of the inflow and by reintroducing the recycled mean profile and fluctuation field. This technique follows those of Kong et al. [4] and Lund et al. [5]. On the other hand, we generate turbulent inflow conditions for the analysis section by exactly copying a turbulent field of the driver section. The parallel and vectorization efficiencies are 98.43% and 99.50%, respectively.

The average of the wall shear stress is at first increased and then decreased with decreasing the wavelength, whilst the pressure drag was gradually increased with decreasing the wavelength (not shown here). In consequence, the trend of the

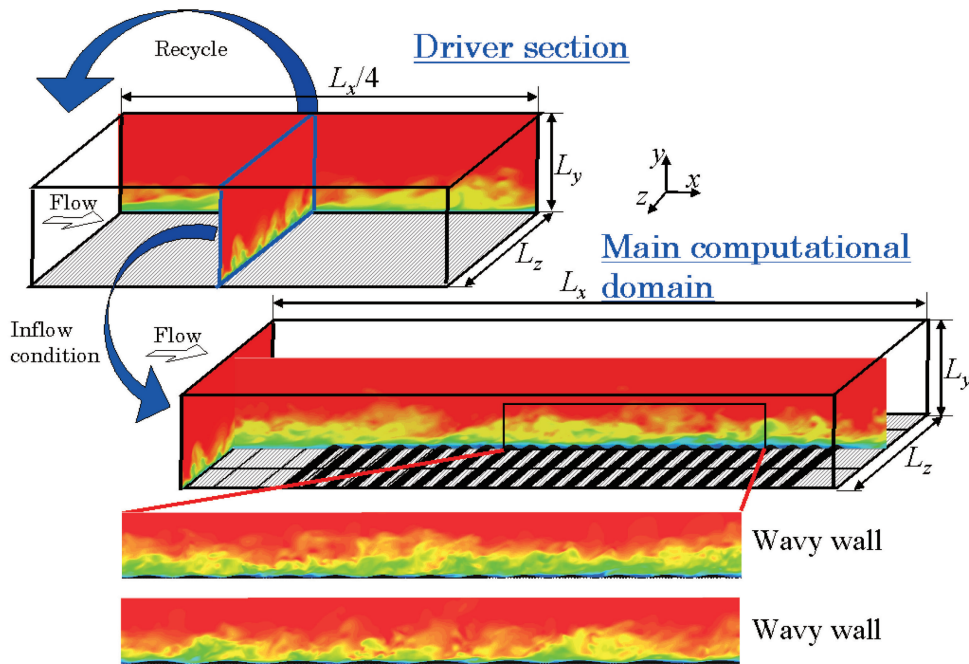


Fig. 2 Computational domains for turbulent boundary layer on several sinusoidal wavy walls.

friction coefficient, which was defined as the summation of the wall shear stress and the pressure drag, is the same as that of the wall shear stress. The friction coefficient is largest at $\lambda/a = 12.5$, which is different from that for the rough wall with transverse square bars [6].

3. Application of LES of turbulent flows to urban environmental and strong wind disaster problems

For the mitigation of heat island effects on coastal cities, it is expected that the sea breeze come into the inland area of a city, where its cold air mingles with the hotter air over and inside the urban canopies. For the numerical simulation of urban heat island, thus far the meteorological model has been

mainly employed, focusing on atmospheric winds in whole range of a city. However, in order to evaluate a local heat environment in such a part of an urban region, it is important to reproduce the complex flows among many buildings and their wakes with smaller scale. Also, for estimating the mitigation of heat island effect by the meteorological local circulation such as a sea breeze, the numerical model that can predict time sequences of unsteady flow quantities is required because the convection brought about by fluctuation behavior of turbulent flows represents directly and strictly an intense and a range of heat transport. Hence, we employ the LES technique for wind flow accompanied with heat around dense tall buildings existing in the urban area. Also, determination of the reference

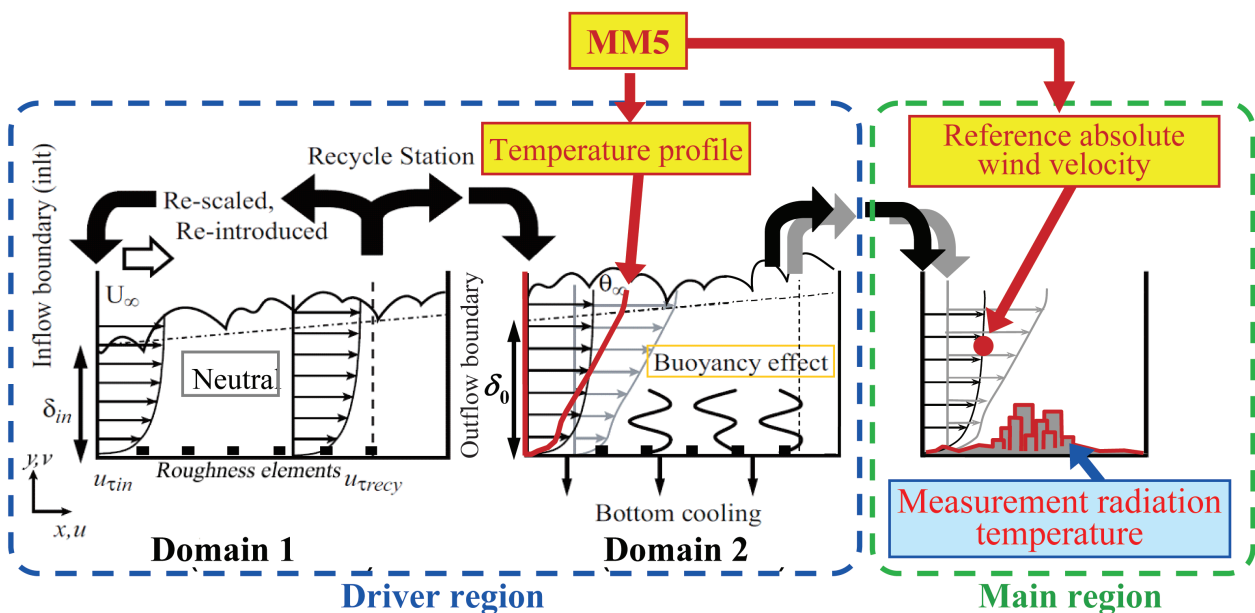


Fig. 3 Hybrid method of Meteorological and LES model.

absolute values for the simulated wind velocity and temperature is supported by the diurnal numerical results obtained by the meso-scale meteorological model (Fig. 3). By comparing with field measurement data, this computational model is validated. Also, we investigate details of a local thermal environment and provide a dominant role of the surface shape and thermal condition of a city from an environmental point of view (Fig. 4).

Recent architectural buildings have a variety of shapes based on unique designer concepts, and the curved surfaces are frequently used for building wall. Here, as a typical and a fundamental case in such buildings, a circular cylinder is focused on. The flow characteristics around a circular cylinder in realistic high Reynolds number region are investigated by use of the LES model. As a result, the present LES model succeeded in simulating the aerodynamic characteristics at the

critical Reynolds numbers. The asymmetric flow characteristics associated with a steady lift are investigated by visualization of the computed data (Figs. 5 and 6).

4. DNS of turbulent heat transfer of non-Newtonian surfactant solution passing complicated geometry

The drag-reducing effect of surfactant additives on turbulent flow has received much attention from both practical and scientific perspectives. This phenomenon can be used for reducing the transportation power in oil-pipeline circuits or district heating and cooling (DHC) recirculation systems: see, for instance, [7]. In general, the surfactant solutions used as working fluids are viscoelastic (non-Newtonian). Their properties measured even in simple shear or extensional flows are known to exhibit appreciably different from those of

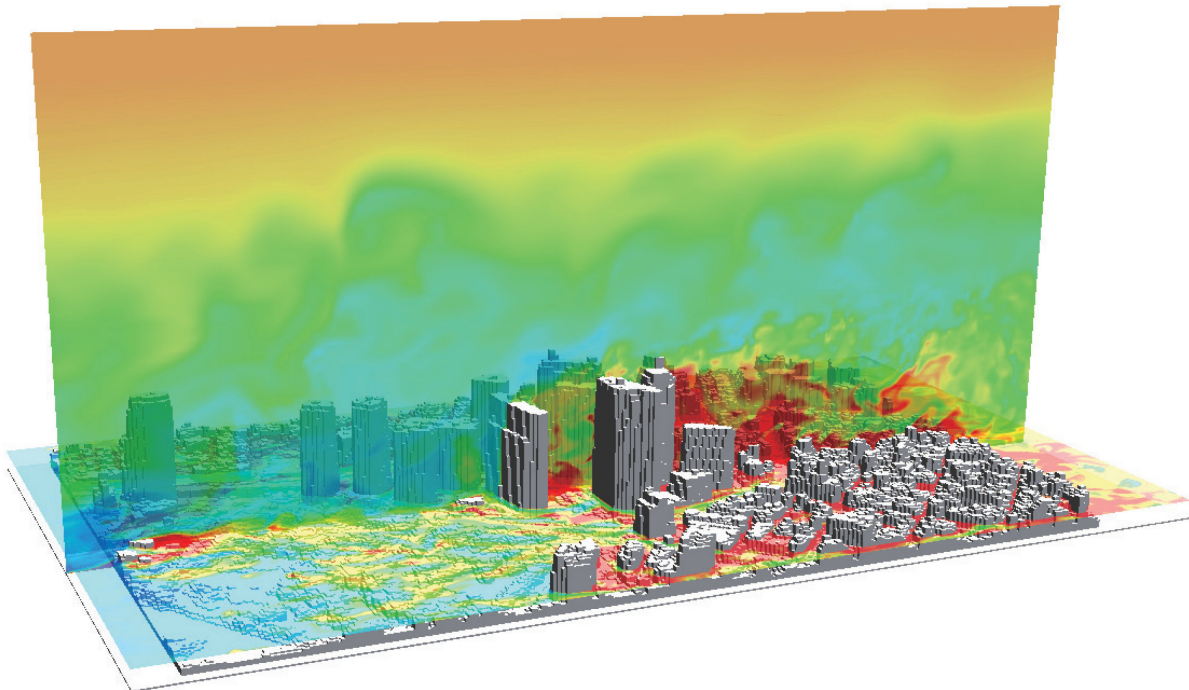


Fig. 4 Instantaneous temperature fields in vertical and horizontal sections of around dense tall buildings.

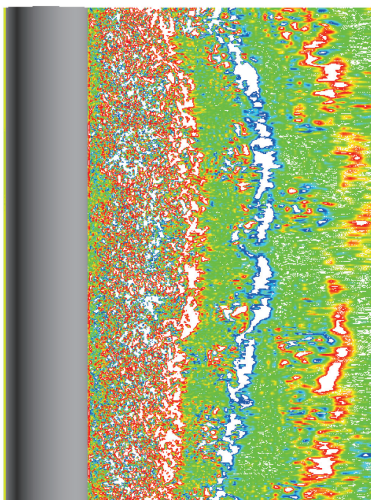


Fig. 5 Wake structures of a circular cylinder ($Re=2 \times 10^5$).

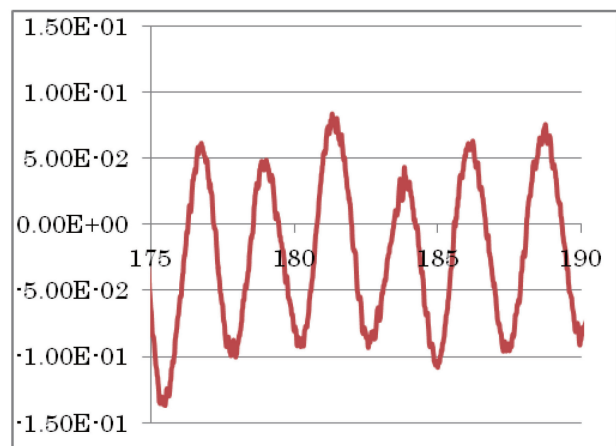


Fig. 6 Time histories of lift coefficients of a circular cylinder ($Re=2 \times 10^5$).

the pure solvent. In addition, as it is known to be a practical problem for heat transport systems, the drag-reducing effect may attenuate the heat transfer significantly due to the suppression of turbulence. In the present study, we addressed this issue and investigated regularly spaced elements (a series of orifices) that induce separation and reattachment and can be applied practically due to their excellent heat transfer performance. Based on Giesekus' viscoelastic-fluid model, DNS of a viscoelastic fluid with passive-scalar heat transfer has been carried out for the same geometry with our previous work [8]. The goal of this work is to better understand the physics and heat-transfer characteristics of the viscoelastic turbulent flow. Major differences between the present study and published works on smooth channels are related to the streamwise variation of the flow state and the main areas where turbulence is produced. Therefore, the instantaneous vortex structures and the relevant momentum and heat transport within the strong shear layer just downstream of the orifice should be explored.

Figure 7 presents a mean-flow field and Reynolds shear-stress distribution with emphasis on the orifice downstream, revealing significant differences between the Newtonian fluid and the viscoelastic fluid. The viscoelastic flow past the orifice expands remarkably due to the normal stress of the fluid elasticity. Thereby the shear layer emanating from the orifice

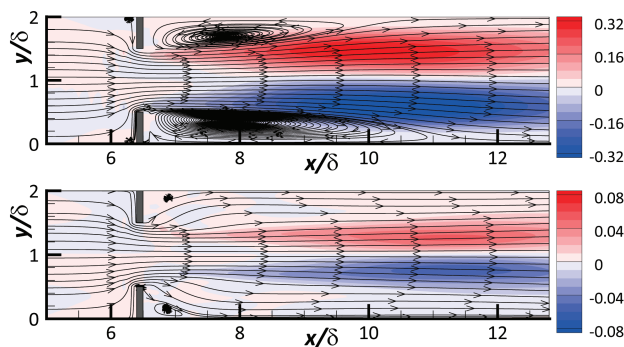


Fig. 7 Averaged streamline and contour of Reynolds shear stress, $\overline{u'v'}$, with emphasis on downstream of the orifice ribs for $Re_{\tau 0} = 30$: (top) Newtonian fluid, (bottom) viscoelastic fluid. The mean flow moves from left to right.

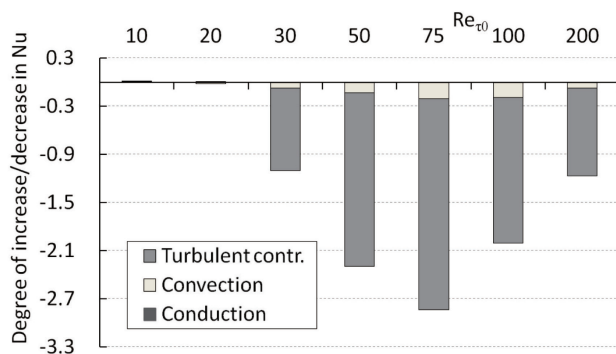


Fig. 8 Decreasing degree in heat transfer for viscoelastic flows: that is, variation of each component contributing to Nusselt number in viscoelastic flows from those of Newtonian flows.

edge and the recirculation zone behind the orifice are found to weaken in the viscoelastic flow, which is almost laminar throughout the channel while the Newtonian flow is turbulent at the same Reynolds number. As a result, the avoiding transition to turbulence gives rise to a heat-transfer reduction as shown in Fig. 8. By increasing the Reynolds number, the reduction of the Nusselt number is pronounced, but becomes less significant gradually for $Re_{\tau 0} > 75$. On the other hand, the magnitude of the drag reduction has a peak at $Re_{\tau 0} = 100$ and still large relative to that of the heat-transfer reduction (figure not shown here). This implies a presence of dissimilarity between drag-reduced flow and thermal field that may be of important practically to develop energy-saving efficient heat exchangers.

References

- [1] K. Morishita, T. Ishihara, and Y. Kaneda, "Small-scale statistics in direct numerical simulation of turbulent channel flow at high-Reynolds number," *Journal of Physics: Conference series*, 318, (2011), 022016.
- [2] Y. Kaneda, T. Ishihara, M. Yokokawa, K. Itakura, and A. Uno, "Energy dissipation rate and energy spectrum in high resolution direct numerical simulations of turbulence in a periodic box," *Physics of Fluids*, 15(2), (2003), L21-L24.
- [3] P. A. Davidson, N. Okamoto, and Y. Kaneda, "On freely-decaying, anisotropic, axisymmetric, Saffman turbulence," *J. Fluid Mech.* (in revision)
- [4] H. Kong, H. Choi, and J.S. Lee, "Direct numerical simulation of turbulent thermal boundary layers," *Phys. Fluids*, 12, (2000), 2555-2568.
- [5] T. S. Lund, X. Wu, and K. D. Squires, "Generation of turbulent inflow data for spatially-developing boundary layer simulations," *J. Comput. Phys.*, 140 (2), (1998), 233–258.
- [6] S. Leonardi, P. Orlandi, R. J. Smalley, L. Djenidi, and R. A. Antonia, "Direct numerical simulations of turbulent channel flow with transverse square bars on one wall," *J. Fluid Mech.*, 491, (2003), 229-238.
- [7] H. Takeuchi, "Demonstration test of energy conservation of central air conditioning system at the Sapporo city office building—Reduction of pump power by flow drag reduction using surfactant," *Synthesiology—English edition*, 4, (2012), 136-143.
- [8] T. Tsukahara, T. Kawase, and Y. Kawaguchi, "DNS of viscoelastic turbulent channel flow with rectangular orifice at low Reynolds number," *International Journal of Heat and Fluid Flow*, 32, (2011), 529-538.

乱流の世界最大規模直接数値計算とモデリングによる応用計算

プロジェクト責任者

金田 行雄 名古屋大学 大学院工学研究科

著者

金田 行雄 名古屋大学 大学院工学研究科

石原 卓 名古屋大学 大学院工学研究科

岩本 薫 東京農工大学 工学府

田村 哲郎 東京工業大学 大学院総合理工学研究科

川口 靖夫 東京理科大学 理工学部

塚原 隆裕 東京理科大学 理工学部

地球シミュレータ (ES2) を用いて、(i) 高レイノルズ数 (壁摩擦速度に基づくレイノルズ数 2560) の平行平板間乱流、(ii) 軸対称の減衰乱流、(iii) 正弦波状壁面上の乱流境界層を含む、カノニカルな問題の大規模直接数値シミュレーション (DNS) を実施した。これらの DNS は、関連する様々な乱流現象に対して詳細で有益な情報を与えるものである。これらの DNS で得られたデータを解析することにより (1) 高レイノルズ数壁乱流の渦度成分の間欠性を示す尖り度などの統計量は壁近傍の特徴的な渦構造と強く関係していること、(2) 軸対称減衰乱流の十分発達した状態において乱流場が等方的にならないこと、(3) 正弦波状の壁における壁乱流の摩擦係数は矩形形状の粗面のある壁における摩擦係数と異なることなどを見出した。また、我々は環境や工学的な応用問題に対する乱流数値計算として、(iv) 実際の都市を対象とした、環境・防災問題の低減化をめざした高解像度大規模乱流のラージ・エディ・シミュレーション (LES)、(v) 近年の多彩な高層ビルを考慮した、円柱周り的高レイノルズ数流れの LES、(vi) 複雑境界を過ぎる非ニュートン流体における乱流熱輸送の DNS を実施した。その結果、(4) 都市部での高層ビル周辺で発生する熱を伴う風の流れに対して、LES の技術を用いて建物間の小規模で複雑な流れを再現できること、(5) LES にて臨界レイノルズ数あたりの円柱周りの流れの空力特性がとらえられること、および、(6) リブ列を有する平行平板間の粘弾性流体乱流においては、滑らかな平行平板間の流れと異なり、熱伝達低減量は抵抗低減効果に比べて小さく、レイノルズ数が増加するにつれてさらに減少していくことが判明した。

キーワード: 大規模直接数値計算, 平行二平板間乱流, 減衰軸対称乱流, 乱流境界層, 粗面, LES, 都市型乱流境界層, 臨界レイノルズ数, 界面活性剤, 熱輸送, 抵抗低減